

Supplemental data

Blocking fatty acid-fueled mROS production within macrophages alleviates acute gouty inflammation

Christopher J. Hall^{1,*}, Leslie E. Sanderson¹, Lisa M. Lawrence¹, Bregina Pool², Maarten van der Kroef¹, Elina Ashimbayeva¹, Denver Britto¹, Jacquie L. Harper³, Graham J. Lieschke⁴, Jonathan W. Astin¹, Kathryn E. Crosier¹, Nicola Dalbeth² and Philip S. Crosier¹.

¹ Department of Molecular Medicine and Pathology, Faculty of Medical and Health Sciences, University of Auckland, Auckland, New Zealand.

² Department of Medicine, Faculty of Medical and Health Sciences, University of Auckland, Auckland, New Zealand.

³ Malaghan Institute for Medical Research, Wellington, New Zealand.

⁴ Australian Regenerative Medicine Institute, Monash University, Victoria, Australia.

* Corresponding author.

Present affiliations:

Leslie E. Sanderson Universite Libre de Bruxelles, Brussels, Belgium

Maarten van der Kroef UMC Utrecht, Netherlands

The authors have declared that no conflict of interests exists.

Corresponding author address:

Christopher J. Hall

Department of Molecular Medicine and Pathology, School of Medical Sciences,

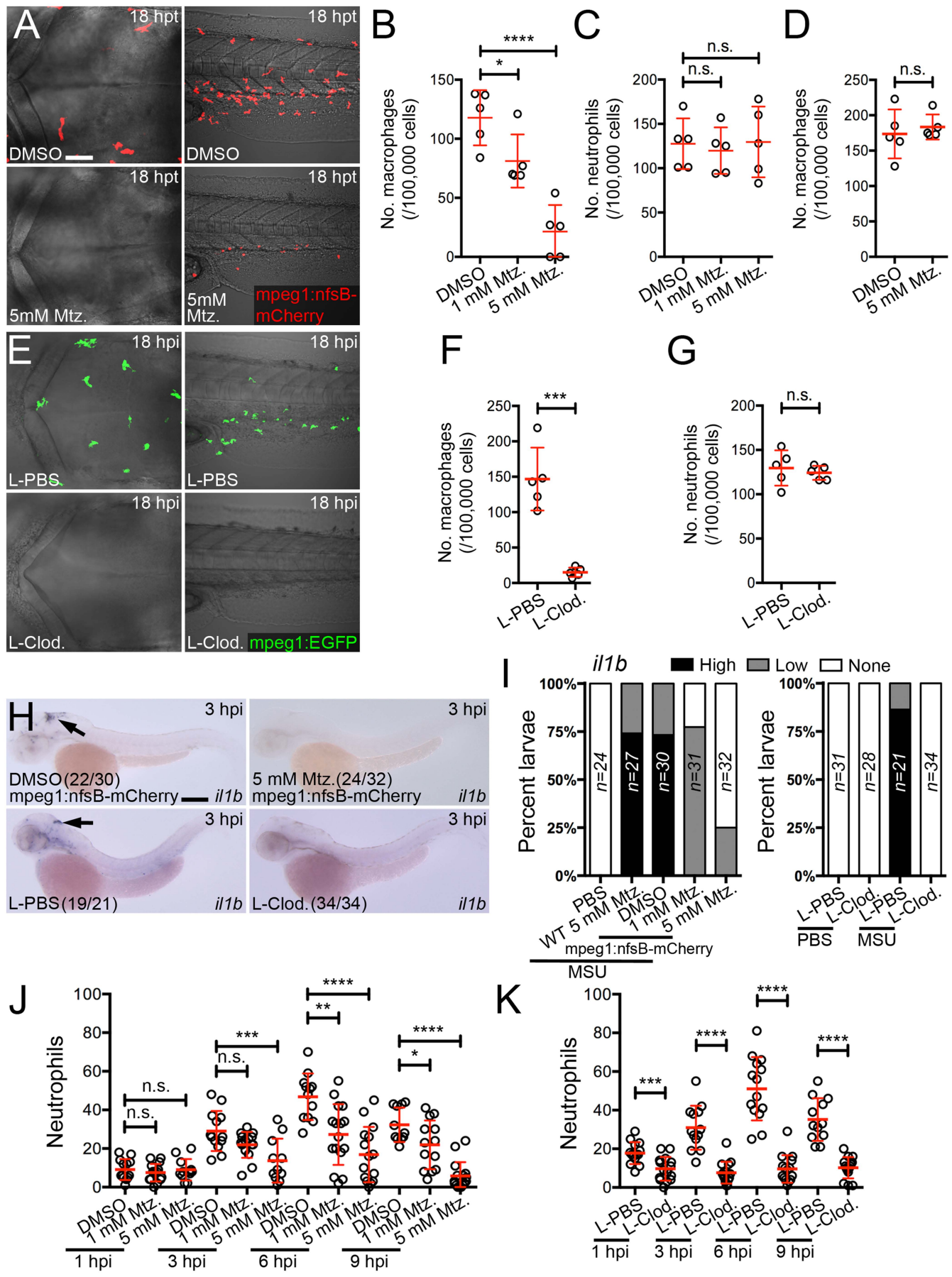
University of Auckland, Private Bag 92019,

Auckland, New Zealand

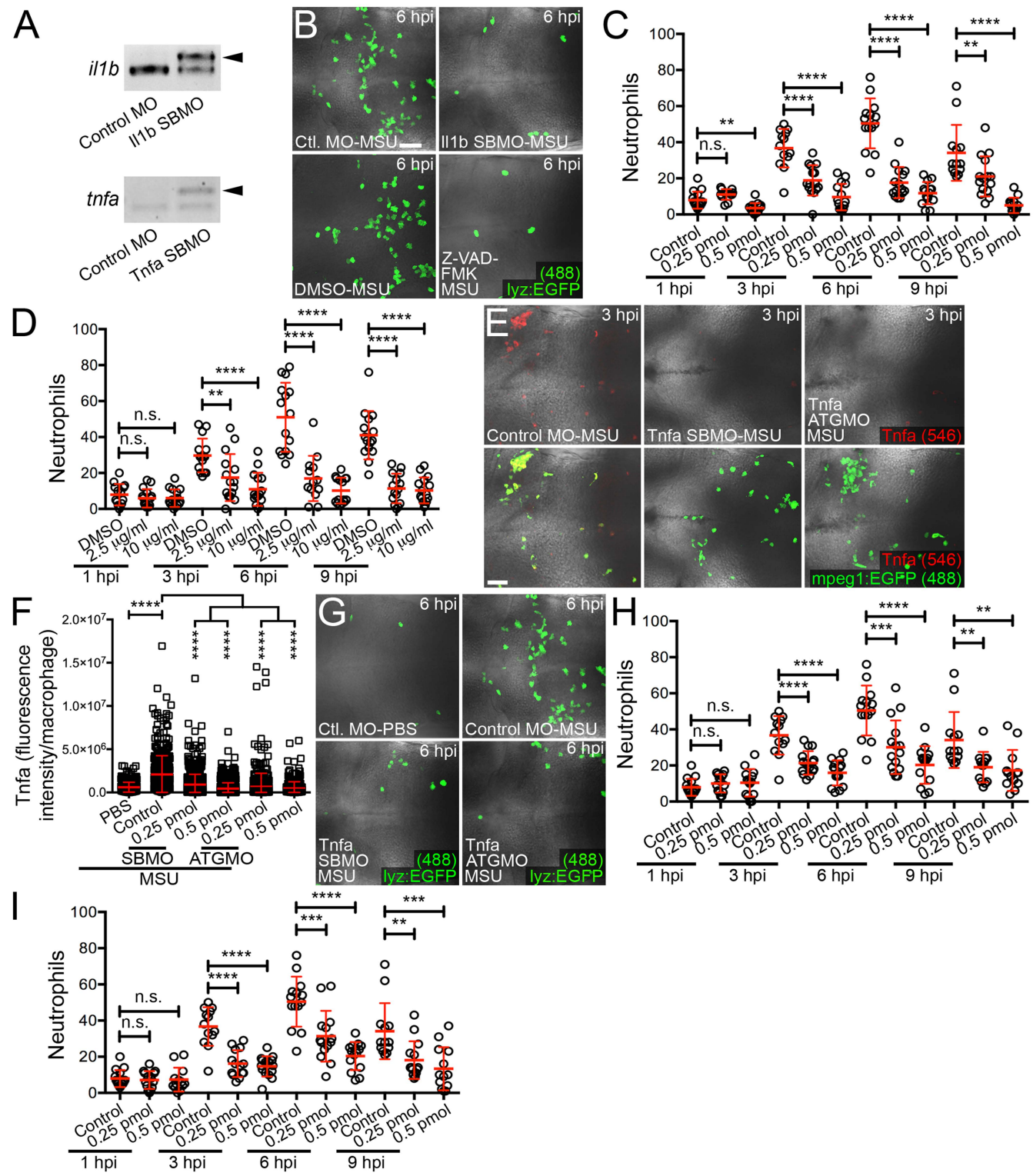
Telephone: +64 9 923 2910

E-mail: c.hall@auckland.ac.nz

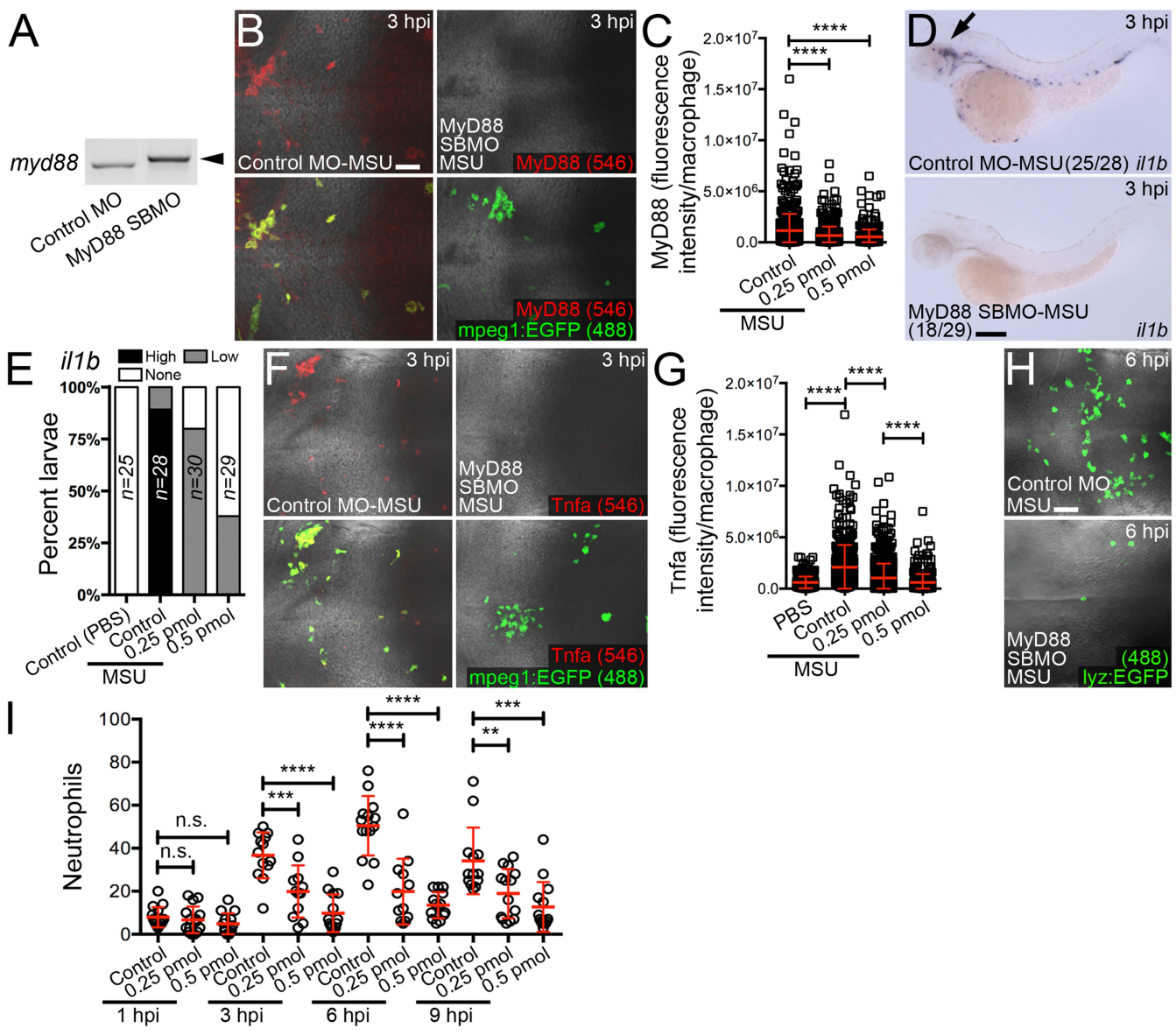
Supplemental Figure 1. MSU crystals activate zebrafish macrophages. (A) Crystal lengths following 18/22 gauge needle dissociation and sonication. (B) Hindbrain expression of *mmp9/krt4* (transverse and dorsal views) within MSU crystal-injected larva (circle, microinjection site). (C) MSU crystal-injected larvae demonstrating 'low' *il1b/irg1* expression (insets, magnified views of hindbrain). (D) Hindbrain macrophage and neutrophil within MSU crystal-injected *Tg(mpeg1:nfsB-mCherry;lyz:EGFP)* larvae (arrow, intracellular crystals). (E) Temporal quantification of crystal phagocytosis, as in D (n=2 larvae). (F) FluoSpheres within hindbrain macrophages (injected into *Tg(mpeg1:nfsB-mCherry)* larvae). (G and I) Expression of *il1b* (G) and *irg1* (I) within PBS-, uric acid-, FluoSphere (F.S.)- and calcium pyrophosphate (CPP) crystal-injected larvae. PBS images in G and I are the same as in Figures 1B and 1D, respectively. (H and J) Temporal quantification of *il1b* (H) and *irg1* (J) expression, as detected in G and I, respectively. (K and L) Flow cytometry quantification of neutrophils within *Tg(lyz:EGFP)* larvae following indicated treatments (K) and MO/CRISPR-Cas9 injections (L), n=~35 larvae/treatment, 5 biological replicates. Untreated sample in panel L is the same as in panel K. Arrows mark *il1b/irg1* expression in hindbrain. Data for D-J pooled from 2 independent experiments. Numbers in parentheses, frequency of larvae with displayed phenotype. All error bars, means \pm SD. **** $P < 0.0001$; n.s., not significant, one-way ANOVA, Dunnett's post hoc test. Scale bars, 50 μm (B), 100 μm (C) and 10 μm (D, F).



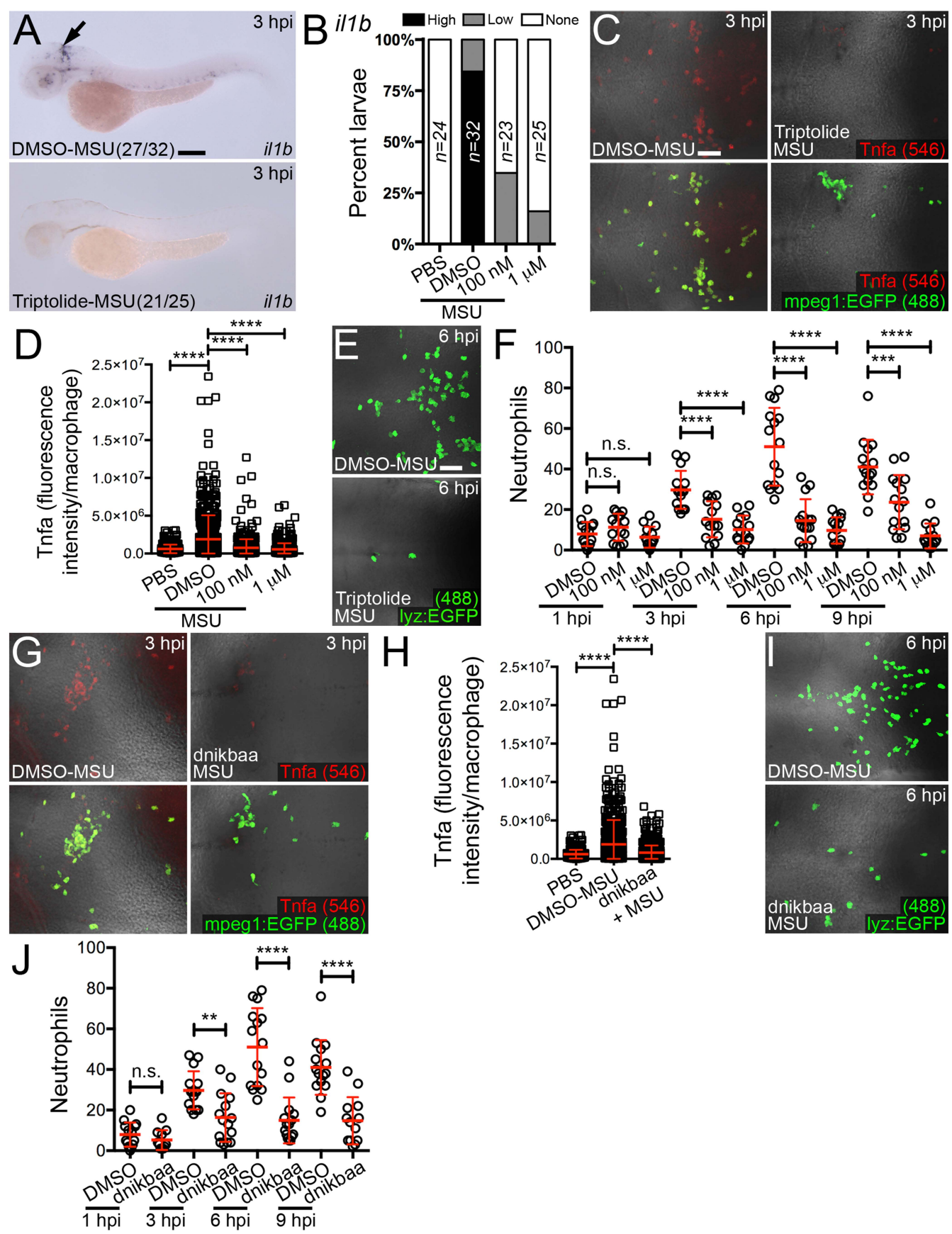
Supplemental Figure 2. MSU crystal-driven neutrophil recruitment is suppressed in macrophage-depleted larvae. (A) Hindbrain and tail of DMSO- and metronidazole (Mtz.)-treated *Tg(mpeg1:nfsB-mCherry)* larvae, 18 hours post treatment (hpt). (B and C) Flow cytometry quantification of macrophages (B) and neutrophils (C) from *Tg(mpeg1:nfsB-mCherry)* (B) and *Tg(lyz:EGFP)* (C) larvae as treated in A. (D) Flow cytometry quantification of macrophages from Mtz.-treated *Tg(mpeg1:EGFP)* larvae. (E) Hindbrain and tail of liposomal PBS (L-PBS)- and liposomal clodronate (L-Clod.)-injected *Tg(mpeg1:EGFP)* larvae, 18 hpi. (F and G) Flow cytometry quantification of macrophages (F) and neutrophils (G) from *Tg(mpeg1:EGFP)* and *Tg(lyz:EGFP)* larvae, respectively, as treated in E. (H) Expression of *il1b* within MSU crystal-injected DMSO- and metronidazole(Mtz.)-treated *Tg(mpeg1:nfsB-mCherry)* larvae and following L-PBS and L-clodronate (L-Clod.) injection. (I) Quantification of *il1b* expression, as detected in H. (J and K) Temporal quantification of neutrophils within the hindbrain of MSU crystal-injected DMSO- and Mtz.-treated *Tg(lyz:EGFP;mpeg1:nfsB-mCherry)* larvae (J) and in L-PBS- and L-clodronate-injected *Tg(lyz:EGFP)* larvae (K), n=13-15 larvae/treatment. For flow cytometry, n=5 groups ~30 larvae/treatment. Arrows mark *il1b* expression in hindbrain. Data for H-K pooled from 2 independent experiments. Numbers in parentheses, frequency of larvae with displayed phenotype. All error bars, means \pm SD. * $P < 0.05$; ** $P < 0.01$; *** $P < 0.001$; **** $P < 0.0001$; n.s., not significant, one-way ANOVA, Dunnett's post hoc test (B, C, J) and Student's *t* test (F, G, K). Scale bars, 50 μm (A) and 100 μm (H).



Supplemental Figure 3. MSU crystal-driven neutrophil recruitment is dependent on macrophage *il1b* expression and *Tnfa* production. (A) RT-PCR for *il1b* and *tnfa* from MSU-injected controlMO-, *Il1b*SBMO- and *Tnfa*SBMO-injected larvae (arrowheads, alternatively spliced transcripts). (B) Immunofluorescence detection of neutrophils within the hindbrain of control MO- and *Il1b* SBMO-injected *Tg(lyz:EGFP)* larvae following MSU crystal injection and MSU crystal-injected DMSO- and Z-VAD-FMK-treated *Tg(lyz:EGFP)* larvae. (C and D) Quantification of neutrophils, as detected in B, for *Il1b* SBMO-injected (C) and Z-VAD-FMK-treated (D) larvae (n=13-15 larvae/treatment). DMSO-MSU samples in panel D are the same as in Figure, 2B/2E/2F. (E) Immunofluorescence of *Tnfa* within controlMO-, *Tnfa*SBMO- and *Tnfa*ATGMO-injected *Tg(mpeg1:EGFP)* larvae following MSU crystal injection. (F) Quantification of *Tnfa*, as detected in E (n=15 larvae/treatment). (G) Immunofluorescence detection of neutrophils within the hindbrain of control MO/PBS-injected and control MO-, *Tnfa* SBMO- and *Tnfa* ATGMO-injected *Tg(lyz:EGFP)* larvae following MSU crystal injection. Control MO-MSU image is the same as in panel B. (H and I) Temporal quantification of neutrophils, as detected in G, for *Tnfa* SBMO-(H) and *Tnfa*ATGMO-(I)injected larvae (n=13-15 larvae/treatment). Control MO-MSU samples are the same as in panel C. Data for B-I pooled from 2 independent experiments. All error bars, means \pm SD. ** $P < 0.01$; *** $P < 0.001$; **** $P < 0.0001$; n.s., not significant, one-way ANOVA, Dunnett's post hoc test. Scale bars, 50 μ m (B, E).

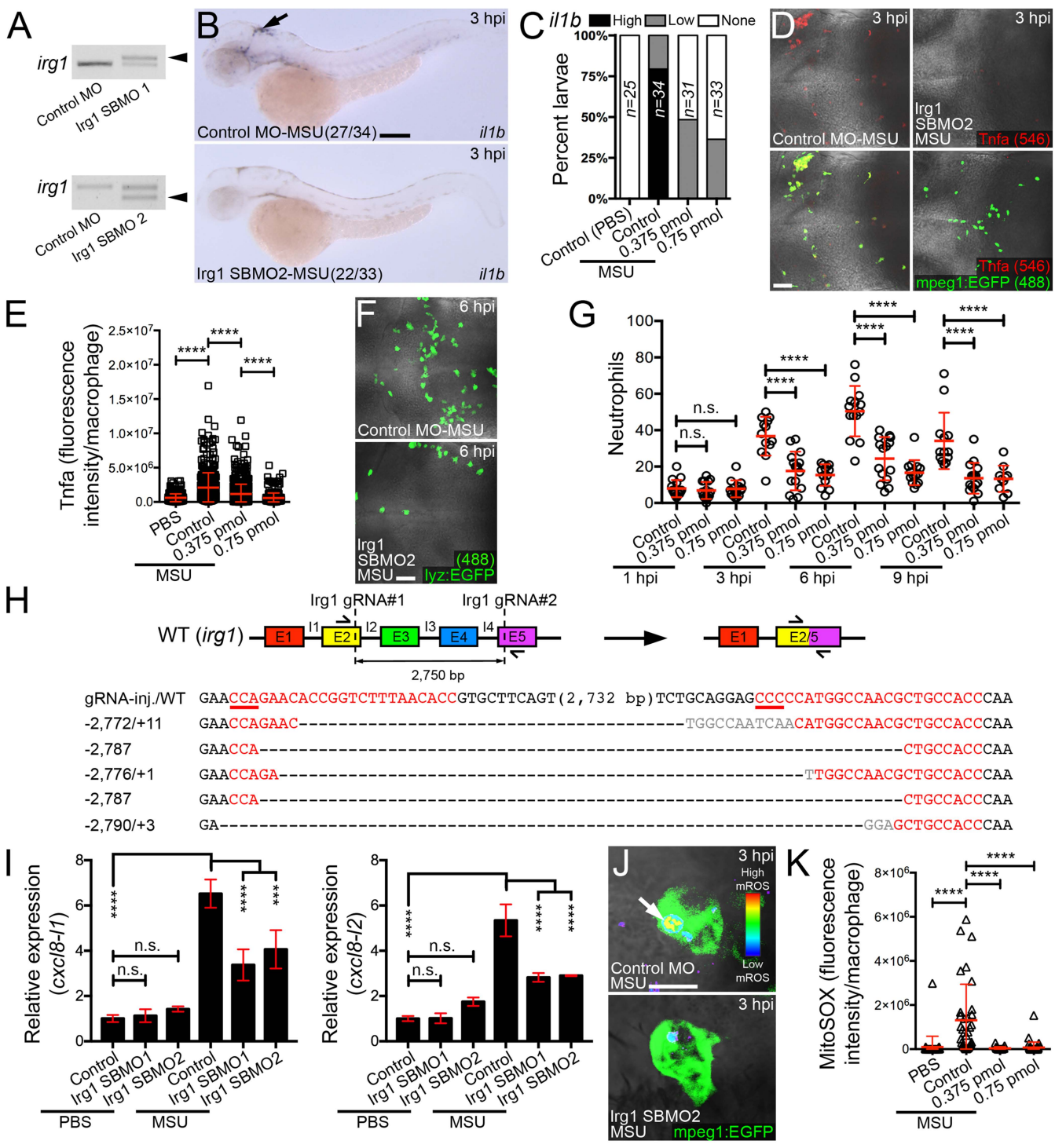


Supplemental Figure 4. MSU crystal-driven macrophage activation and neutrophil recruitment is dependent on MyD88. (A) RT-PCR for *myd88* from MSU crystal-injected control MO- and MyD88SBMO-injected larvae (arrowhead, alternatively spliced transcript). (B) Immunofluorescence of MyD88 within control MO- and MyD88SBMO-injected *Tg(mpeg1:EGFP)* larvae following MSU crystal injection. (C) Quantification of MyD88, as detected in B (n=15 larvae/treatment). (D) Expression of *il1b* within control MO-, and MyD88SBMO-injected larvae following MSU crystal injection. (E) Quantification of *il1b* expression, as detected in D. (F) Immunofluorescence of *Tnfa* within control MO- and MyD88SBMO-injected *Tg(mpeg1:EGFP)* larvae following MSU crystal injection. Control MO-MSU image is the same as in Supplemental Figure 3E. (G) Quantification of *Tnfa*, as detected in F (n=15 larvae/treatment). Control MO-MSU sample is the same as in Supplemental Figure 3F. (H) Immunofluorescence detection of neutrophils within control MO- and MyD88SBMO-injected *Tg(lyz:EGFP)* larvae following MSU crystal injection. Control MO-MSU image is the same as in Supplemental Figure 3B/3G. (I) Quantification of neutrophils, as detected in H (n=13-15 larvae/treatment). Control MO-MSU samples are the same as in Supplemental Figure 3C/3H/3I. Arrow marks *il1b* expression in hindbrain. Data for B-I pooled from 2 independent experiments. Numbers in parentheses, frequency of larvae with displayed phenotype. All error bars, means \pm SD. ** $P < 0.01$; *** $P < 0.001$; **** $P < 0.0001$; n.s., not significant, one-way ANOVA, Dunnett's post hoc test. Scale bars, 50 μ m (B, H) and 100 μ m in (D).



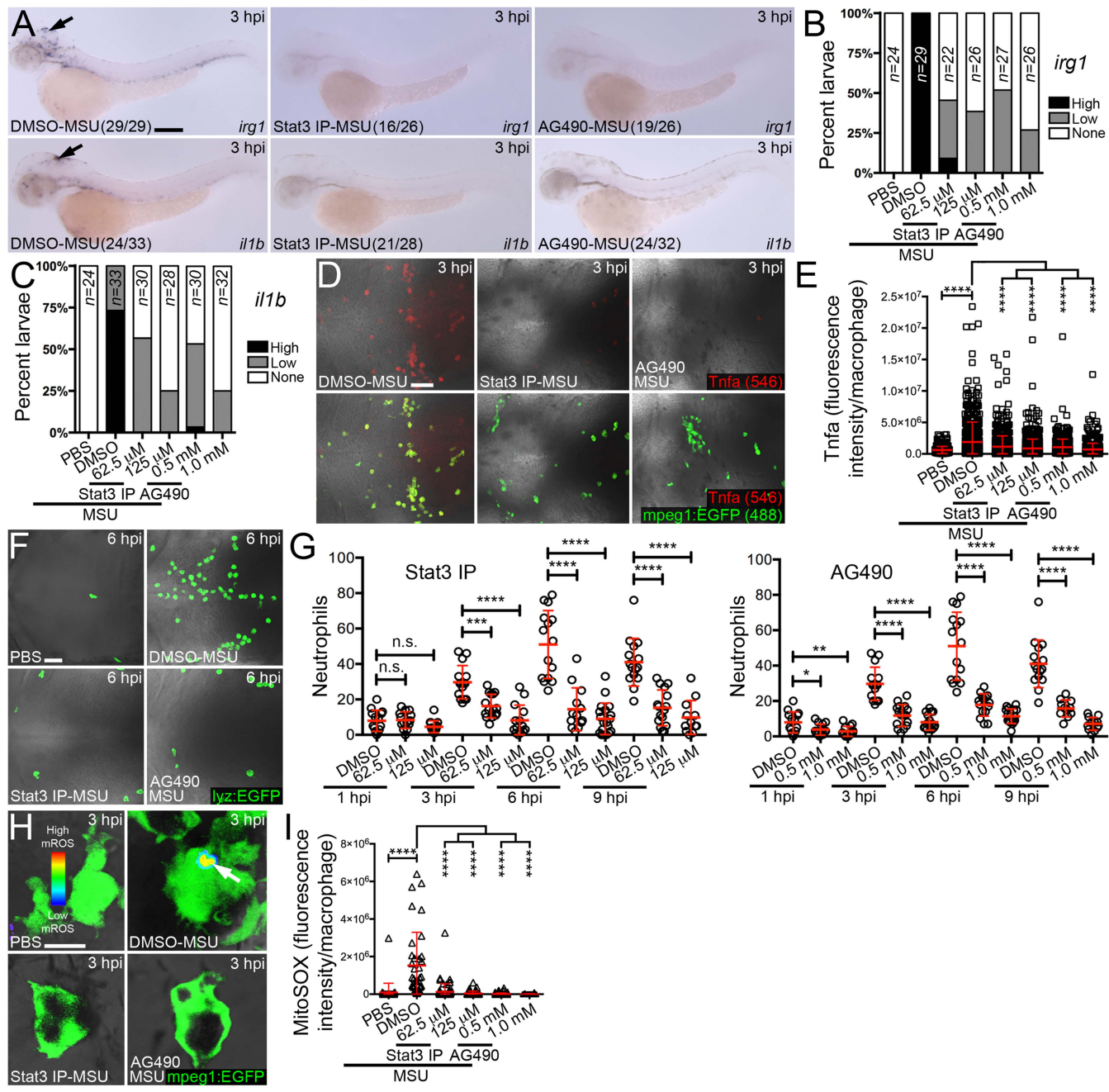
Supplemental Figure 5. Blocking NF- κ B signaling suppresses MSU crystal-driven macrophage activation and neutrophil recruitment. (A) Expression of *il1b* within MSU-injected DMSO-, and triptolide-treated larvae. DMSO-MSU image is the same as in Figure 3A. (B) Quantification of *il1b* expression, as detected in A. DMSO-MSU sample is the same as in Figure 3B. (C) Immunofluorescence of *Tnfa* within MSU crystal-injected DMSO- and triptolide-treated *Tg(mpeg1:EGFP)* larvae. DMSO-MSU image is the same as in Figure 3C. (D) Quantification of *Tnfa*, as detected in C (n=15 larvae/treatment). DMSO-MSU sample is the same as presented in Figures 1G (3 hpi)/3D. (E) Immunofluorescence detection of neutrophils within MSU crystal-injected DMSO- and triptolide-treated *Tg(lyz:EGFP)* larvae. DMSO-MSU image is the same as in Figure 4A and Supplemental Figure 3B. (F) Quantification of neutrophils, as detected in E (n=13-15 larvae/treatment). DMSO-MSU samples are the same as in Figures, 2B/2E/2F/4B/4C and Supplemental Figure 3D. (G) Immunofluorescence of *Tnfa* within the hindbrain of MSU crystal-injected DMSO-treated and *mpeg1:dnikbaa*-injected *Tg(mpeg1:EGFP)* larvae. (H) Quantification of *Tnfa*, as detected in G (n=15 larvae/treatment). DMSO-MSU sample is the same as in panel D and Figures 1G (3 hpi)/3D. (I) Immunofluorescence detection of neutrophils within the hindbrain of DMSO-treated and *mpeg1:dnikbaa*-injected *Tg(lyz:EGFP)* larvae following MSU crystal injection. DMSO-MSU image is the same as in Figure 2D. (J) Temporal quantification of neutrophils, as detected in I (n=13-15 larvae/treatment). DMSO-MSU samples are the same as in panel F, Figure 2B/2E/2F and Supplemental Figure 3D. Arrow marks *il1b* expression in

hindbrain. All data pooled from 2 independent experiments. Numbers in parentheses, frequency of larvae with displayed phenotype. All error bars, means \pm SD. ** $P < 0.01$; *** $P < 0.001$; **** $P < 0.0001$; n.s., not significant, one-way ANOVA, Dunnett's post hoc test (D, F, H) and Student's t test (J). Scale bars, 100 μm in (A) and 50 μm (C, E).



Supplemental Figure 6. *Irg1* contributes to MSU crystal-driven macrophage activation and neutrophil recruitment. (A) RT-PCR for *irg1* from control MO-, *Irg1* SBMO1- and *Irg1* SBMO2-injected larvae following MSU crystal injection (arrowheads, alternatively spliced transcripts). (B) Expression of *il1b* within control MO- and *Irg1* SBMO2-injected larvae following MSU crystal injection. Control MO-MSU image is the same as in Figure 5A. (C) Quantification of *il1b* expression, as detected in B. Control MO-MSU sample is the same as in Figure 5B. (D) Immunofluorescence of *Tnfa* within the hindbrain of control MO- and *Irg1* SBMO2-injected *Tg(mpeg1:EGFP)* larvae following MSU crystal injection. Control MO-MSU image is the same as in Figure 5D and Supplemental Figures 3E/4F. (E) Quantification of *Tnfa*, as detected in D (n=15 larvae/treatment). Control MO-MSU sample is the same as in Figure 5E and Supplemental Figures 3F/4G. (F) Immunofluorescence detection of neutrophils within the hindbrain of control MO- and *Irg1* SBMO2-injected *Tg(lyz:EGFP)* larvae following MSU crystal injection. Control MO-MSU image is the same as in Figure 6A and Supplemental Figures 3B/3G/4H. (G) Temporal quantification of neutrophils, as detected in F (n=13-15 larvae/treatment). Control MO-MSU samples are the same as in Figure 6B and Supplemental Figures 3C/3H/3I/4I. (H) Target sites for *Irg1* gRNAs#1/2 and examples of deletions detected by sequencing amplicons generated from individual gRNA/cas9-injected larvae using highlighted primers, compared to gRNA-only-injected larvae (-/+), deletions and additions [in grey], respectively). I, intron; E, exon; red sequence, gRNA targets (PAM sequence underlined). (I) Expression of *cxcl8-11* and *cxcl8-12* within control MO-, *Irg1* SBMO1 and *Irg1*

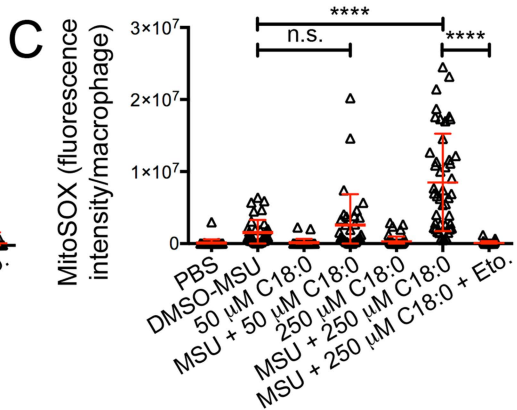
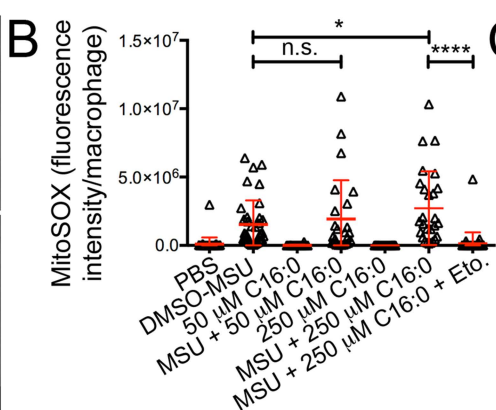
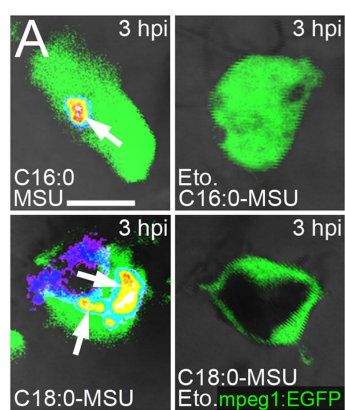
SBMO2-injected larvae following PBS and MSU crystal injection (as detected by qPCR at 3 hpi, n=25-30 larvae per sample, 3 biological replicates). (J) Macrophage mROS production (white arrow) within the hindbrain of control MO- and Irg1 SBMO2-injected *Tg(mpeg1:EGFP)* larvae following MSU crystal injection (MitoSOX signal displayed as a heatmap, warmer colors represents higher levels of mROS). Control MO-MSU image is the same as in Figure 6D. (K) Quantification of macrophage-specific mROS production, as detected in J (n=10 larvae/treatment). Control MO-MSU sample is the same as in Figure 6E. Black arrow marks *il1b* expression in hindbrain. Data for B-G and J,K pooled from 2 independent experiments. Numbers in parentheses, frequency of larvae with displayed phenotype. Error bars, means \pm SD. *** $P < 0.001$; **** $P < 0.0001$; n.s., not significant, one-way ANOVA, Dunnett's post hoc test. Scale bars, 100 μm (B), 50 μm (D, F) and 10 μm (J).



Supplemental Figure 7. JAK/STAT signaling contributes to macrophage activation and neutrophil recruitment in response to MSU crystals. (A) Expression of *irg1* and *il1b* within MSU crystal-injected DMSO-, Stat3 inhibitor peptide(Stat3 IP)- and AG490-treated larvae. (B and C) Quantification of *irg1* (B) and *il1b* (C) expression, as detected in A. (D) Immunofluorescence of *Tnfa* within the hindbrain of MSU crystal-injected DMSO-, Stat3 IP- and AG490-treated *Tg(mpeg1:EGFP)* larvae. DMSO-MSU image is the same as in Figure 3C and Supplemental Figure 5C. (E) Quantification of *Tnfa*, as detected in D (n=15 larvae/treatment). DMSO-MSU sample is the same as in Figures 1G (3 hpi)/3D/5F and Supplemental Figures 5D/5H. (F) Immunofluorescence detection of neutrophils within the hindbrain of PBS-injected and MSU crystal-injected DMSO-, Stat3 IP- and AG490-treated *Tg(lyz:EGFP)* larvae. PBS image is the same as in Figure 4A. (G) Temporal quantification of neutrophils, as detected in F (n=13-15 larvae/treatment). DMSO-MSU samples are the same as in Figures, 2B/2E/2F/4B/4C/6C and Supplemental Figures 3D/5F/5J. (H) Macrophage mROS production (white arrow) within the hindbrain of MSU crystal-injected DMSO-, Stat3 IP- and AG490-treated *Tg(mpeg1:EGFP)* larvae (MitoSOX signal displayed as a heatmap, warmer colors represents higher levels of mROS). (I) Quantification of macrophage-specific mROS production, as detected in H (n=10 larvae/treatment). DMSO-MSU sample is the same as in Figure 6F. Black arrows mark *irg1/il1b* expression in hindbrain. All data pooled from 2 independent experiments. Numbers in parentheses, frequency of larvae with displayed phenotype. All error bars, means \pm SD. * $P < 0.05$; ** $P < 0.01$; *** $P < 0.001$;

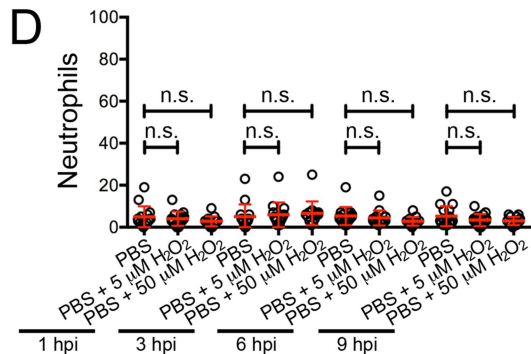
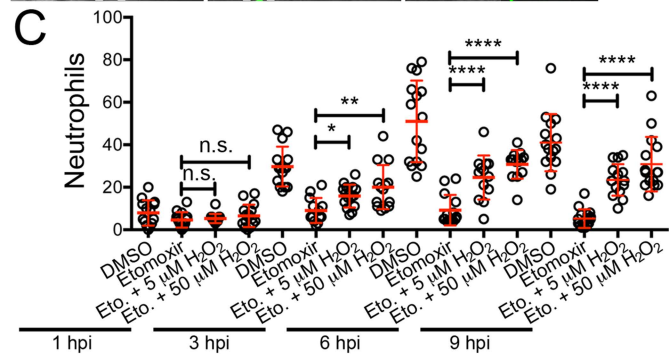
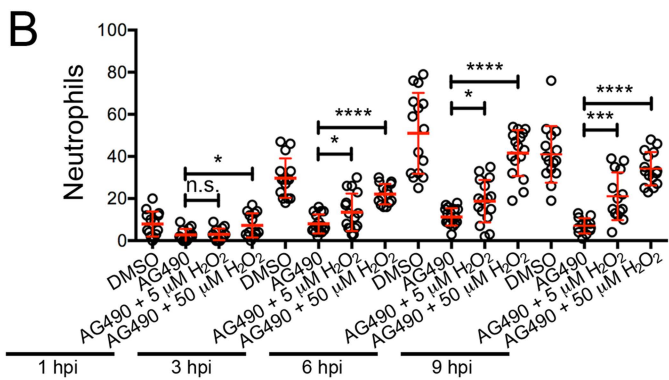
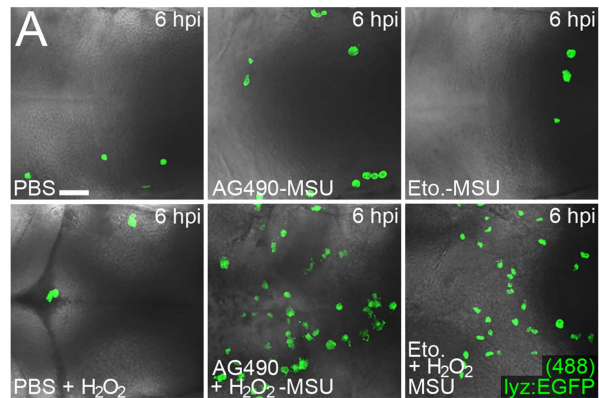
**** $P < 0.0001$; n.s., not significant, one-way ANOVA, Dunnett's post hoc test.

Scale bars, 100 μm (A), 50 μm (D, F) and 10 μm (H).

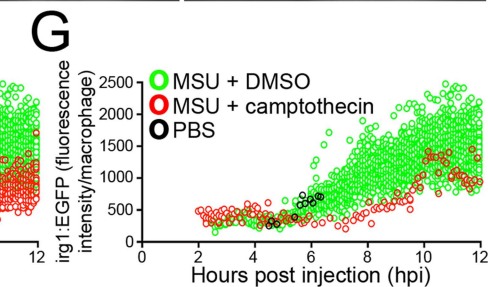
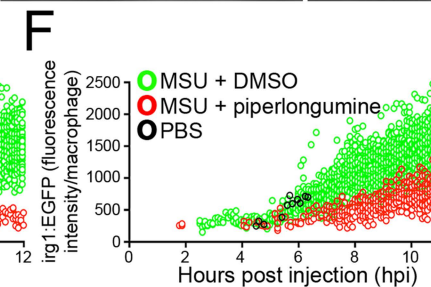
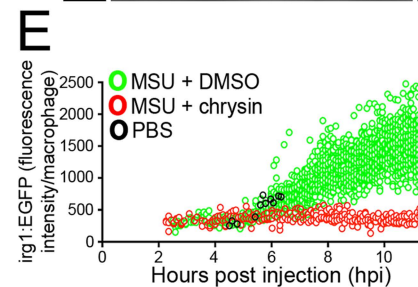
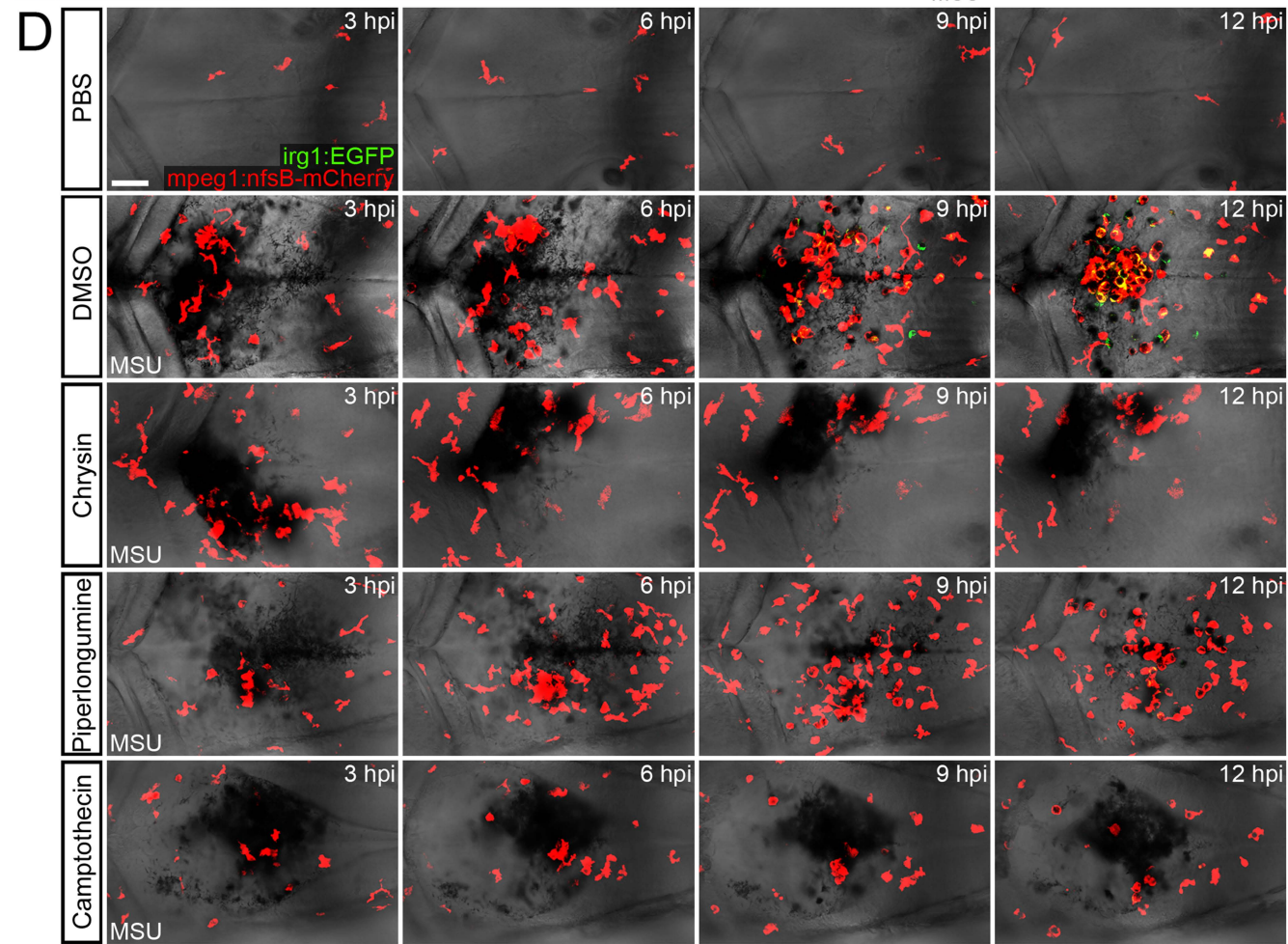
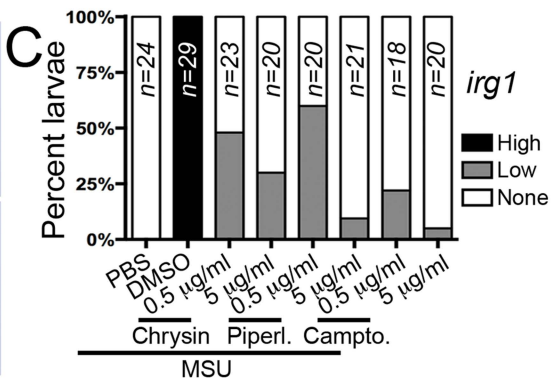
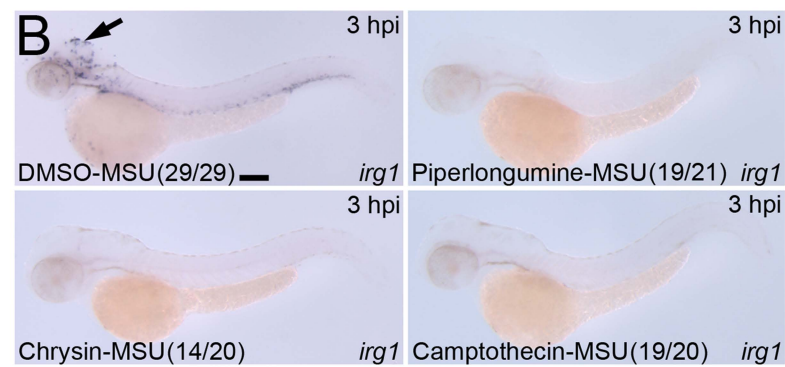
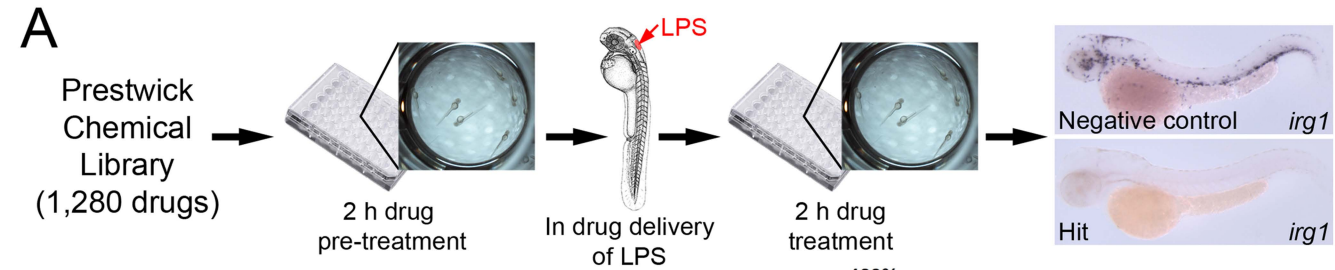


Supplemental Figure 8. Hindbrain injection of C16:0 or C18:0 elevates MSU crystal-driven macrophage-specific mROS production through a FAO-dependent mechanism. (A) Live imaging of macrophage mROS production within the hindbrain of *Tg(mpeg1:EGFP)* larvae co-injected with MSU crystals and C16:0 or C18:0 with and without etomoxir (Eto.) treatment. (B and C) Quantification of macrophage-specific mROS production, as detected in A, for C16:0 (B) and C18:0 (C) treatments (n=10 larvae/treatment). DMSO-MSU samples are the same as in Figures 6F/8E and Supplemental Figure 7I. All data pooled from 2 independent experiments. All error bars, means \pm SD. * P <0.05; **** P <0.0001; n.s., not significant, one-way ANOVA, Dunnett's post hoc test. Scale bar, 10 μ m (A).

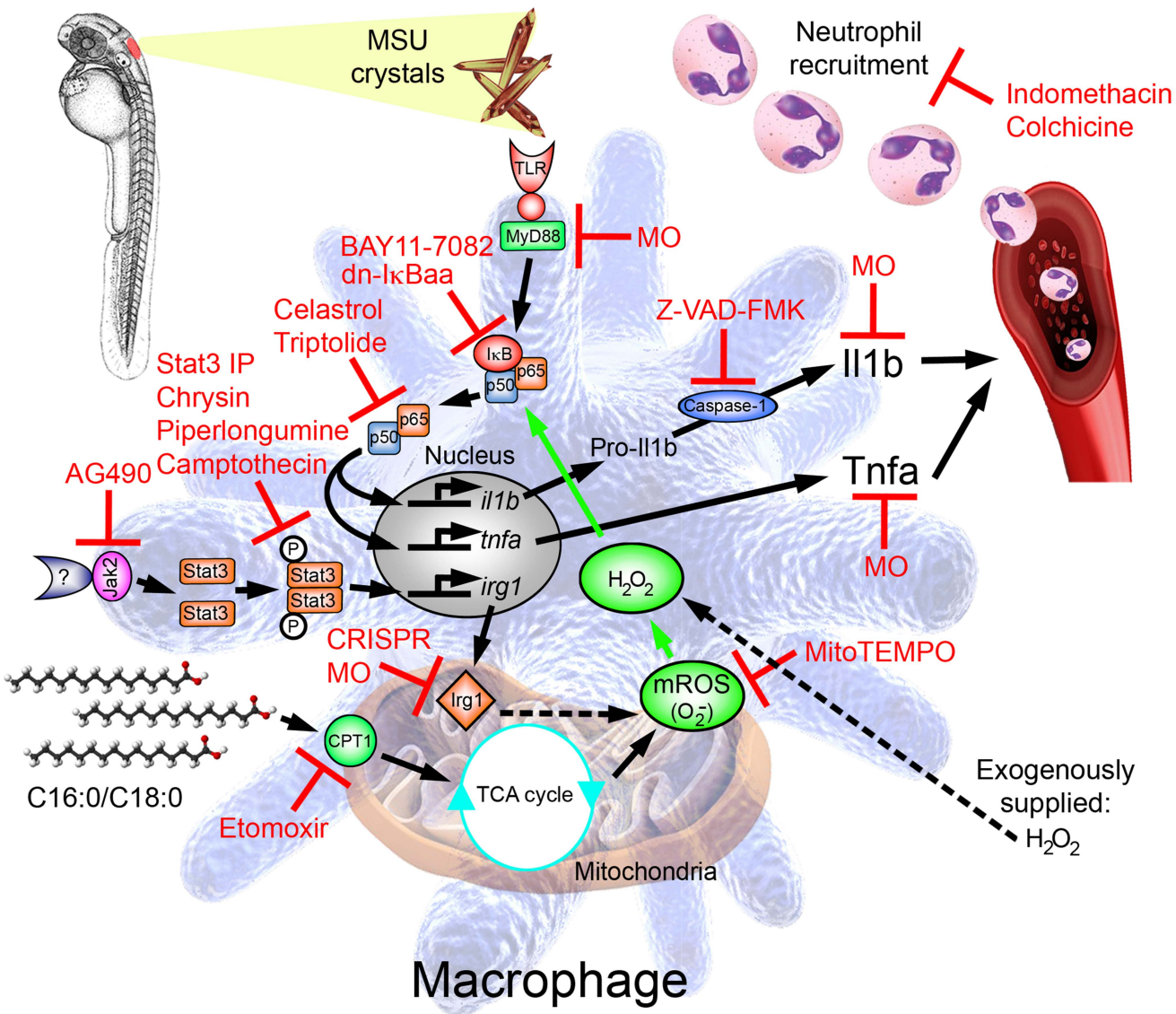
Supplemental Figure 9. Exogenous H₂O₂ can rescue MSU crystal-driven macrophage activation following endogenous mROS depletion. (A) Schematic showing delivery of exogenously supplied H₂O₂ to the hindbrain region and ratiometric HyPer imaging of H₂O₂ levels (488/405 nm ratio is displayed as a heat map, with warmer colors representing higher levels of H₂O₂) within the hindbrain region of *HyPer* mRNA-injected larvae 5 min before (-5 min post injection, mpi) and after (5 and 90 mpi) injection of 50 μM H₂O₂. (B) Expression of *il1b* within PBS-injected (with and without co-injected 50 μM H₂O₂) and MSU crystal-injected AG490(1 mM)- and etomoxir(Eto., 250 μM)-treated (with and without co-injected 50 μM H₂O₂) larvae. PBS image is the same as in Figures 1B/7A and Supplemental Figure 1G. (C) Quantification of *il1b* expression, as detected in B. DMSO-MSU sample is the same as in Figure 10E. (D) Immunofluorescence of *Tnfa* within the hindbrain of PBS/H₂O₂(50 μM)-injected *Tg(mpeg1:EGFP)* larvae and MSU crystal-injected AG490(1.0 mM)- and etomoxir(250 μM)-treated larvae, with and without co-injected 50 μM H₂O₂. (E) Quantification of *Tnfa*, as detected in D (n=15 larvae/treatment). DMSO-MSU sample is the same as in Figures 1G (3 hpi)/3D/5F/7D/11B and Supplemental Figures 5D/5H/7E. Arrows mark *il1b* expression in hindbrain. Data for B-E pooled from 2 independent experiments. Numbers in parentheses, frequency of larvae with displayed phenotype. All error bars, means ± SD. **P*<0.05; ***P*<0.01; *****P*<0.0001; n.s., not significant, one-way ANOVA, Dunnett's post hoc test. Scale bars, 100 μm (A, B) and 50 μm (D).



Supplemental Figure 10. Exogenous H₂O₂ can rescue MSU crystal-driven neutrophil recruitment following endogenous mROS depletion. (A) Immunofluorescence detection of neutrophils within the hindbrain of PBS-injected *Tg(lyz:EGFP)* larvae (with and without co-injected 50 μM H₂O₂) and MSU crystal-injected AG490(1.0 mM)- and etomoxir(250 μM)-treated larvae (with and without co-injected 50 μM H₂O₂). PBS image is the same as in Figure 8A. (B and C) Quantification of neutrophils, as detected in A, for AG490/H₂O₂- (B) and etomoxir/H₂O₂- (C) treatments (n=13-15 larvae/treatment). DMSO-MSU samples are the same as in Figures, 2B/2E/2F/4B/4C/6C/8B/8C/11D/11E and Supplemental Figures 3D/5F/5J/7G. (D) Quantification of neutrophils, as detected in A, for PBS/H₂O₂-treatments (n=13-15 larvae/treatment). All data pooled from 2 independent experiments. All error bars, means ± SD. **P*<0.05; ***P*<0.01; ****P*<0.001; *****P*<0.0001; n.s., not significant, one-way ANOVA, Dunnett's post hoc test. Scale bar, 50 μm (A).



Supplemental Figure 11. Phenotypic drug screen uncovers chrysin, piperlongumine and camptothecin as inhibitors of *irg1* expression in activated macrophages. (A) Schematic of drug screen to uncover repurposed drugs that suppress *irg1* expression in activated macrophages. (B) Expression of *irg1* within MSU crystal-injected DMSO-, chrysin-, piperlongumine- and camptothecin-treated larvae. DMSO-MSU image is the same as in Supplemental Figure 7A. (C) Quantification of *irg1* expression, as detected in B. DMSO-MSU sample is the same as presented in Supplemental Figure 7B. (D) Time-lapse confocal imaging of macrophage activation (EGFP expression within mCherry⁺ macrophages) within the hindbrain of MSU crystal-injected DMSO-, chrysin-, piperlongumine- and camptothecin-treated *Tg(irg1:EGFP;mpeg1:nfsB-mCherry)* larvae. (E-G) Quantification of macrophage activation (measured as fluorescence intensity of EGFP within individual mCherry⁺ macrophages), as detected in D, within PBS-, MSU crystal + DMSO-, MSU crystal + chrysin- (E), MSU crystal + piperlongumine- (F) and MSU crystal + camptothecin-treated (G) *Tg(irg1:EGFP;mpeg1:nfsB-mCherry)* larvae. MSU + DMSO and PBS samples are the same in panels E-G. Arrow marks *irg1* expression in hindbrain. Data for B and C pooled from 2 independent experiments. Numbers in parentheses, frequency of larvae with displayed phenotype. Scale bars, 100 μ m (B) and 50 μ m (D).



Supplemental Figure 12. Model of Irg1-dependent, FAO/mROS-driven activation of macrophages in response to MSU crystals. Pharmacologic and genetic interventions used in this study to support this model are shown in red.

Supplemental Figure 13. Comparisons between control groups used in this study. (A) Control groups used when assessing the effects of pharmacologic treatments (DMSO), genetic depletion of macrophages (mpeg1:nfsB/DMSO), liposomal clodronate-mediated depletion of macrophages (L-PBS) and MO-mediated depletion studies (Control MO) on the temporal recruitment of neutrophils following MSU crystal injection (n=13-15 larvae/treatment). DMSO-MSU samples are the same as in Figures, 2B/2E/2F/4B/4C/6C/8B/8C/11D/11E/13B-D and Supplemental Figures 3D/5F/5J/7G/10B/10C. mpeg1:nfsB/DMSO and L-PBS samples are the same as in Supplemental Figure 2J and 2K, respectively. Control MO samples are the same as in Figure 6B and Supplemental Figures 3C/3H/3I/4I/6G. (B) Control groups used when assessing the effects of pharmacologic treatments (DMSO) and MO-mediated depletion studies (Control MO) on macrophage-specific Tnfa production following MSU crystal injection (n=15 larvae/treatment). DMSO-MSU sample is the same as in Figures 1G (3 hpi)/3D/5F/7D/11B/12D and Supplemental Figures 5D/5H/7E/9E. Control MO-MSU sample is the same as in Figure 5E and Supplemental Figures 3F/4G/6E. (C) Control groups used when assessing the effects of pharmacologic treatments (DMSO) and MO-mediated depletion studies (Control MO) on macrophage-specific mROS production (MitoSOX signal) following MSU crystal injection (n=10 larvae/treatment). DMSO-MSU sample is the same as in Figures 6F/8E/13F and Supplemental Figures 7I/8B/8C. Control MO-MSU sample is the same as in Figure 6E and Supplemental Figure 6K. All data pooled from 2 independent experiments. All

error bars, means \pm SD. **** $P < 0.0001$; n.s., not significant, one-way ANOVA, Dunnett's post hoc test.